Smart Helmet: Monitoring Brain, Cardiac and Respiratory Activity

Wilhelm von Rosenberg[1], Theerasak Chanwimalueang[1],
Valentin Goverdovsky[1], Danilo P. Mandic[1]

Abstract— **The timing of the assessment of the injuries following a road-traffic accident involving motorcyclists is absolutely crucial, particularly in the events with head trauma. Standard apparatus for monitoring cardiac activity is usually attached to the limbs or the torso, while the brain function is routinely measured with a separate unit connected to the head-mounted sensors. In stark contrast to these, we propose an integrated system which incorporates the two functionalities inside an ordinary motorcycle helmet. Multiple fabric electrodes were mounted inside the helmet at positions featuring good contact with the skin at different sections of the head. The experimental results demonstrate that the R-peaks (and therefore the heart rate) can be reliably extracted from potentials measured with electrodes on the mastoids and the lower jaw, while the electrodes on the forehead enable the observation of neural signals. We conclude that various vital sings and brain activity can be readily recorded from the inside of a helmet in a comfortable and inconspicuous way, requiring only a negligible setup effort.**

I. Introduction

Wearable devices are set to revolutionise and democratise personalised diagnosis and treatment, bringing it to millions, if not billions of people. Monitoring health in extreme situations is essential to ensure the safety and to provide rapid response in the event of emergencies. To this end, it is a prerequisite to obtain accurate measurements of vital signs and brain activity as soon as possible even if no external or obvious signs of trauma are present. As a preventive measure, recordings of cardiac and brain activity enable the examination and assessment of stress and concentration levels, which are especially important in potentially dangerous situations such as flying a plane, riding a motorcycle or skiing. Common parameters that are considered for the evaluation of the physiological state are body temperature, heart rate, breathing rate and blood pressure [1]. Additionally, the electroencephalogram (EEG) can provide an indication of the psychological state of a person. This proof-of-concept study illuminates the feasibility of performing measurements from the sensors mounted inside a helmet worn while executing a set of specific activities. This work uses a modified motorcycle helmet. However, the techniques and approaches described are applicable to all helmets for which their inner lining is in good contact with the skin at a number of locations on the head.

Some of the previous work in this area include measurements of the electrocardiogram (ECG) of Formula 1 drivers during races [2] employing electrodes attached to the torso which had to be installed before every event. However, a system that can be set up off-site or does not require a laborious setup process would be beneficial as it reduces the inconvenience for the person being examined [3]. Obtaining a ballistocardiogram and a single lead ECG from sensors placed behind the ear [4] showed the possibility to collect cardiac data non-invasively from head locations. Additionally, the ECG and electrooculogram (EOG) were recorded from an army helmet equipped with electrodes attached to straps [5], and the ECG between both ears from modified earphones [6]. Another ear-based recording technique is in-the-ear EEG where an EEG is obtained from electrodes inside the ear canals [7].

Although similar to this work none of the above approaches demonstrated an integrated solution for monitoring both brain and body functions simultaneously. Other improvements of the proposed method and apparatus compared to the earlier work are: (i) the increased comfort and convenience since the helmet is worn in the same way as a standard helmet; and (ii) the enhanced performance achieved by the steady electrode-skin contact. A precursor of this study is described in [8], where cardiac data were extracted from electrodes underneath a motorcycle helmet using metallic gold cup electrodes. In the current study, the rigid electrodes were replaced with flexible conductive fabric and the cardiac data were supplemented with measurements of the brain activity. This fabric can be easily integrated within the inner lining of a helmet and requires only saline solution to achieve the low impedance contact. We have analysed the potential differences between the electrodes and the optimal sensor positions. The utility of the cardiac data obtained from the helmet was corroborated with the reference signal recorded simultaneously from the limbs, while the capabilities of the proposed system to measure the brain function were verified for standard brain responses – auditory steady state response (ASSR) and steady-state visual evoked potential (SSVEP).

II. Experimental Details

A. Background

Heartbeats are triggered by electrical currents propagating through the heart. From a distance, the superposition of all current dipoles in the entire heart can be represented by one electric dipole – the heart vector – for which the orientation and amplitude change over the course of one cycle. In this study we investigate six electrode positions: two to monitor brain and four to monitor cardiac activity. Comparing with standard ECG electrode configurations, the setup is approximately akin to lead I [9]. However, the

[1]Department of Electrical and Electronic Engineering, Imperial College London, United Kingdom {wv12, tc2113, goverdovsky, d.mandic}@ic.ac.uk

978-1-4244-9270-1/15/$31.00 ©2015 IEEE

currents produced in the heart travel through inhomogeneous tissues and geometries until they are picked up by sensors on the head. Therefore, they may include components of other standard leads and are likely to be corrupted by artefacts such as cheek and jaw movements and other muscle activity.

The most prominent feature of the ECG cycle is the R-peak – a sharp spike with a high amplitude. Its occurrences in time can be used to determine the heart rate. To be able to assess the quality of the recordings, the identified timings of R-peaks are compared to reference measurements taken from the arms and quantified using the established parameters: sensitivity (Se) and positive predictivity ($+P$) [10]:

$$Se = \frac{TP}{TP + FN} \quad (1) \qquad +P = \frac{TP}{TP + FP} \quad (2)$$

where *TP* stands for the number of correctly identified R-peaks, *FN* for the number of missed R-peaks and *FP* for the number of points incorrectly labelled as R-peaks. Furthermore, we introduce another measure of quality, that of assessing the deviation of the estimated heart rate from the actual heart rate at regular instances in time.

There is a number of EEG paradigms, particularly evoked response potentials (ERP), which lend themselves well to testing new hardware. The two we have concentrated on in this work are the SSVEP and the ASSR. SSVEP is the signal that originates in the visual cortex [11] in response to a visual stimulus operating at a fixed rate of $3.5\,\mathrm{Hz}$ to $75\,\mathrm{Hz}$. The resulting brain electrical activity contains exactly the same or multiples of the stimulation frequency. It is widely used in the area of brain computer interfaces (BCI) due to excellent signal-to-noise (SNR) ratio and robustness to artefacts. ASSR involves the hearing pathway and is the brain's response to auditory stimuli. When presented with either white noise or a high frequency sinusoidal signal (e.g. $1\,\mathrm{kHz}$) amplitude modulated with another sinusoid of significantly lower frequency (e.g. $40\,\mathrm{Hz}$), the human brain 'demodulates' the signal and produces the response at the modulating frequency [12]. This response is most pronounced in the temporal lobe of the brain. We have evaluated the performance of the two forehead electrodes by analysing the recordings during the exposure of the subjects to the above two stimuli. Additionally, we have also assessed the capability of the setup to measure the alpha rhythm – periodic signal bursts in the $7.5\,\mathrm{Hz}$ – $15.5\,\mathrm{Hz}$ frequency band, produced by the brain in a relaxed state especially with eyes closed.

B. Setup

A standard motorcycle helmet was equipped with electrodes mounted on its inner lining (see Fig. 1 (left)). Conductive fabric (MedTex130) was used to construct the electrodes, ensuring that they are unobtrusive and fit well inside the helmet. The fabric electrodes can easily be sewed directly into the helmet cloth at a later stage and the results are expected to be identical. However, the ability to freely move electrodes around was more important at this stage. The electrode positions were chosen based on the quality of the contact with the skin and their location relative to the sources of the signals of interest. Out of seven electrodes, three were in contact with the forehead, the one in the centre serving as the common ground (GND), two on the mastoids, and two on both sides of the lower jaw, see Fig. 1 (right). They are named after the side on the head – **L**eft or **R**ight, and their position – **F**orehead, **M**astoid or **J**aw. To reduce the impedance of the electrode-skin interface, the fabric was lightly wetted with saline solution.

The two electrodes on the sides of the forehead (LF and RF) recorded brain activity and the potentials were measured relative to the LJ electrode, while LF acted as a reference for potential measurements at the other four locations (LM, RM, LJ and RJ). Impedances between GND and the signal channels ranged from $4\,\mathrm{k\Omega}$ to $16\,\mathrm{k\Omega}$ for subject 1 and from $9\,\mathrm{k\Omega}$ to $32\,\mathrm{k\Omega}$ for subject 2. The unipolar setup enabled the measurement of potential differences between any two channels which is useful in the analysis of ECG recordings. To establish the ground truth, ECG was also recorded between the two arms. Data were acquired from two different subjects for $60\,\mathrm{s}$ to $300\,\mathrm{s}$ at a sampling rate of $1200\,\mathrm{S/s}$ using the bio-signal amplifier – g.USBamp (g.tec) and analysed in retrospect. The experimental procedures involving human subjects described in this paper were approved by the Institutional Review Board.

For both ECG and EEG measurements the subjects were engaged in three different scenarios while sitting at rest: (i) awake with eyes close – alpha rhythm measurement; (ii) listening to a $1\,\mathrm{kHz}$ sinusoid, amplitude-modulated with a $40\,\mathrm{Hz}$ sinusoid – ASSR measurement; and (iii) attending an LED blinking at a rate of $15\,\mathrm{Hz}$ – SSVEP measurement.

III. Data Preprocessing

A. ECG channels

As mentioned before, the electrical model of the heart can be represented as a dipole for which the potential differences are the largest when the two measurement points are at the opposite ends of the dipole. However, the geometry of the human body is not regular and the orientation of the heart vector changes over time, therefore, the potential differences for all six channel combinations of LM, RM, LJ and RJ were considered and analysed to identify the most suitable ones.

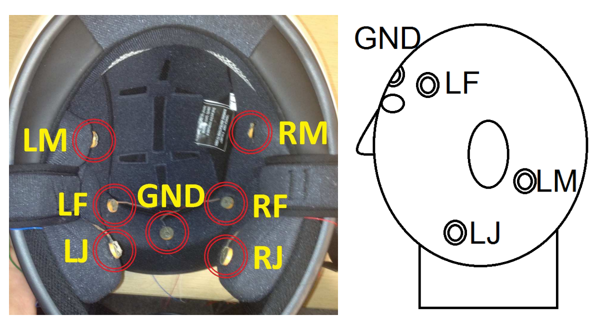

Fig. 1. Setup of the helmet (left) and the positions of the electrodes on the head (right).

This study concentrates on the accuracy of the heart rate, thus only the timings of the R-peaks were important and the selection of the filter parameters did not take into account the need to preserve any of the other characteristics of the ECG waveform. Generally established methods which identify particular characteristics of the ECG-cycle do not seem to be optimised for signals with consistently high levels of noise. For example, the algorithm developed in [13] attains very good values for Se (as defined above), but due to a large number of false positives, the values for $+P$ are low for most channels. In [8] R-peak identification success rates were compared after applying various static bandpass filters to ECG signals with very low SNR. Experimentally it was found that 3rd order Butterworth bandpass filters with cut-off frequencies around $8\,\mathrm{Hz}$ and $25\,\mathrm{Hz}$ lead to the best results. This filter configuration corresponds to the frequencies necessary to represent the R-peak having a duration of $0.04\,\mathrm{s}$ (minimum period where the amplitude of the R-peak is above the baseline) to $0.12\,\mathrm{s}$ (maximum length of the QRS complex) [14]). Meanwhile, other details of the ECG-cycle (such as the P- and T-peak) are lost after such filtering. Subsequently, the resulting signals were scanned for R-peaks and the identified timings were compared to the actual occurrences from ground truth recordings measured at the arms which have high SNR. Thus, R-peak locations can be easily validated visually. The R-peak search in the signals was performed by determining local peaks separated by a minimum time and with an amplitude above a certain threshold.

B. EEG channels

The potentials measured at the forehead electrodes, LF and RF, were preprocessed according to the brain response of interest. In scenario (i) – alpha rhythm measurement – a 4th order Butterworth filter with a bandpass range between $1\,\mathrm{Hz}$ and $30\,\mathrm{Hz}$ was applied. For scenarios (ii) and (iii), the lower cut-off of the bandpass filter was kept constant at 1 Hz and the upper cut-off was set to $45\,\mathrm{Hz}$ and $25\,\mathrm{Hz}$, respectively.

IV. Discussion

A. Cardiac activity

The accuracy of the R-peak detection was quantified using two different methods with the parameters Se and $+P$ as outlined in Section II and by calculating the deviation of the estimated heart rate from the real heart rate measured from the arms. An R-peak is classified as correctly identified if it occurs within $[t_R - \Delta t, t_R + \Delta t]$ where t_R is the time of the actual R-peak and $\Delta t = 0.02 \times \Delta t_{RR}$, with Δt_{RR} being the average time between two adjacent R-peaks. Depending on the position of the sensors and therefore the angle between the vector connecting the two points and the heart vector, the most significant peak in the ECG cycle can occur with a slight time offset to the standard measurement from the arms. To avoid classifying identified peaks as incorrect even though they exhibit a constant positive or negative delay, another parameter is introduced – the heart rate measure obtained from the inverse of the duration of five full ECG cycles.

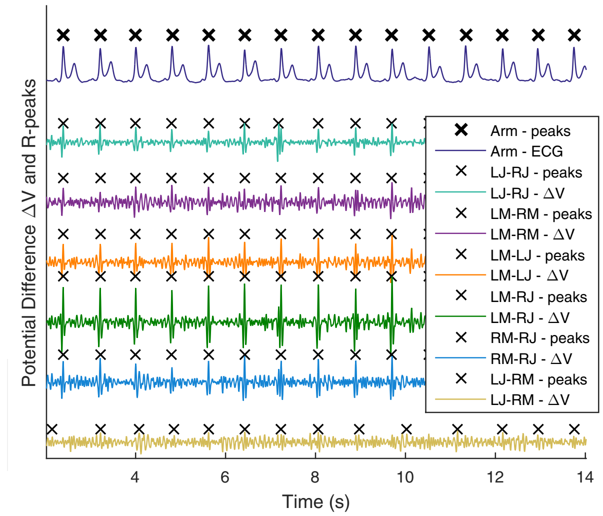

Fig. 2. Potential differences measured between electrodes on the face (lines) and identified R-peaks (crosses) compared to a reference ECG from the arms (top trace).

We quantify the accuracy of this measure as the root-mean-square error (RMSE) of the heart rate deviation (HRD) – the difference between the estimated and the real heart rate at every second. The results are shown in TABLE I where the total number of R-peaks across multiple subjects and trials was 1289 and the HRD was measured in beats per minute (bpm).

For subject 1, the sensor combinations LJ-RJ, LM-LJ, LM-RJ, and RM-RJ produced very reliable signals across all trials. The values for Se and $+P$ were close to 100% and the HRD was less than 1. The LM-LJ, the LM-RJ and in most trials also the LJ-RJ show approximately the same results for the 2nd subject. However, the signal quality of the other channels is much lower. This is also reflected in TABLE I which summarises the results across all subjects and trials with LM-LJ and LM-RJ featuring the best performance parameters. Varying outcomes for certain electrode combinations across trials can be explained by a disturbed connection between at least one of the electrodes and the skin, e.g. in one of the trials for subject 2 all measurements which include RM did not result in reliable extractions of R-peaks. A poor performance of a particular electrode pair in general can indicate that the two electrodes involved are

TABLE I

Quality of the recordings assessed in sensitivity (Se), positive predictivity (+P) and heart rate deviation (HRD).

Setup	TP	FN	FP	Se	+P	HRD (bpm)
LJ-RJ	1211	79	72	93.9%	94.4%	2.28
LM-RM	791	499	605	61.3%	56.7%	11.26
LM-LJ	1275	15	15	98.8%	98.8%	0.66
LM-RJ	1278	12	12	99.1%	99.1%	0.80
RM-RJ	1071	219	253	83.0%	80.9%	6.41
LJ-RM	516	774	977	40.0%	34.6%	17.02

positioned on equipotential lines with very similar values for a significant part of the ECG cycle. To further improve the results, particularly in low SNR scenarios, the detection of R-peaks can be enhanced in software by combining multiple signals during the R-peak search.

B. Brain activity

Three standard brain responses were investigated: (i) ASSR, (ii) alpha rhythm and (iii) SSVEP and the results are shown on Fig. 3. The power spectral density (PSD) was calculated using Welch's method with the window overlap of 80% and the window length of 4.8 seconds for (ii) and the window length of 12 seconds for (i) and (iii).

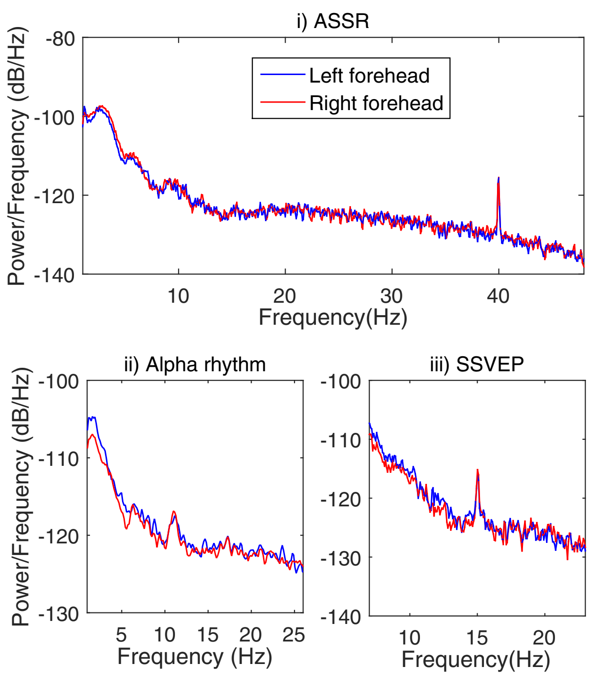

Fig. 3. Power spectra of three different brain responses: i) ASSR at 40 Hz; ii) Alpha rhythm; and iii) SSVEP at 15 Hz.

All scenarios were measured on both subjects using the two electrodes on the forehead – LF and RF. As outlined in section II, an increased power is expected at the frequency of the amplitude-modulating signal (40 Hz) for case (i). The exact frequency band for the alpha rhythm in (ii) varies between people and is normally between 7.5 Hz and 15.5 Hz. A visual stimulus in case (iii) at 15 Hz triggers a brain response at the same frequency. In Fig. 3 (i) the characteristic ASSR is clearly recognisable. Fig. 3 (ii) exhibits the above baseline power level around 10 Hz and 12 Hz – the so called alpha-band – indicating presence of the alpha rhythm. The SSVEP at the frequency of the LED-stimulus in the third trial is demonstrated in Fig. 3 (iii), with a sharp peak in the spectrum at 15 Hz.

V. Conclusion

Existing approaches to heart rate detection from within a commercially available helmet employ wet gel electrodes attached directly to the skin. This proof-of-concept study has demonstrated that this is also achievable with fabric electrodes mounted on the helmet, thereby significantly simplifying the setup and making the system more user-friendly. Combined with the estimation of the respiratory effort from the heart rate variability [15], [8] the proposed approach has made it possible to record the vital signs – heart rate, respiration, and brain activity – from the head in an unobtrusive and convenient way.

To increase the amount of information about the state the body and mind of a person, the follow-on work will include monitoring eye blinking and its effects in recordings at LF and RF since for example the frequency of eye blinks is related to drowsiness. Moreover, other conductive materials that do not require the application of a saline solution to reduce the impedance of the skin-electrode interface will be examined. Finally, studies will be performed while riding in traffic.

References

[1] M. R. Neuman, "Measurement of vital signs: Temperature," *IEEE Pulse*, vol. 1, no. 2, pp. 40–49, 2010.

[2] R. Bedini, A. Belardinelli, G. Palagi, M. Varanini, A. Ripoli, S. Berti, C. Carpeggiani, F. Paone, and R. Ceccarelli, "ECG telemetric evaluation in formula one drivers," in *Proceedings of the IEEE International Conference on Computers in Cardiology*, 1995, pp. 353–356.

[3] A. Casson, D. Yates, S. Smith, J. Duncan, and E. Rodriguez-Villegas, "Wearable electroencephalography," *IEEE Engineering in Medicine and Biology Magazine*, vol. 29, no. 3, pp. 44–56, 2010.

[4] D. Da He, E. S. Winokur, and C. G. Sodini, "A continuous, wearable, and wireless heart monitor using head ballistocardiogram (BCG) and head electrocardiogram (ECG)," in *Proceedings of the IEEE International Conference on Engineering in Medicine and Biology Society (EMBC)*, 2011, pp. 4729–4732.

[5] Y. S. Kim, J. M. Choi, H. B. Lee, J. S. Kim, H. J. Baek, M. S. Ryu, R. H. Son, and K. S. Park, "Measurement of biomedical signals from helmet based system," in *Proceedings of the IEEE International Conference on Engineering in Medicine and Biology Society (EMBS)*, 2007, pp. 359–362.

[6] T. Shen, T. Hsiao, Y. Liu, and T. He, "An ear-lead ECG based smart sensor system with voice biofeedback for daily activity monitoring," in *Proceedings of the IEEE International Region 10 Conference (TENCON)*, 2008, pp. 1–6.

[7] D. Looney, P. Kidmose, C. Park, M. Ungstrup, M. L. Rank, K. Rosenkranz, and D. P. Mandic, "The In-the-Ear recording concept: User-centered and wearable brain monitoring," *IEEE Pulse*, vol. 3, no. 6, pp. 32–42, 2012.

[8] W. von Rosenberg, T. Chanwimalueang, D. Looney, and D. P. Mandic, "Vital signs from inside a helmet: A multichannel face-lead study," in *Proceedings of the IEEE International Conference on Acoustics, Speech and Signal Processing (ICASSP)*, vol. TBC, 2015, p. TBC.

[9] K. M. Lewis and K. A. Handal, *Sensible analysis of the 12-lead ECG*, ser. Allied Health Series. Delma/Thomson Learning, 2000.

[10] B. Köhler, C. Hennig, and R. Orglmeister, "The principles of software QRS detection," *IEEE Engineering in Medicine and Biology Magazine*, vol. 21, no. 1, pp. 42–57, 2002.

[11] H. Strasburger, W. Scheidler, and I. Rentschler, "Amplitude and phase characteristics of the steady-state visual evoked potential," *Applied Optics*, vol. 27, no. 6, pp. 1069–1088, 1988.

[12] R. Galambos, S. Makeig, and P. J. Talmachoff, "A 40-Hz auditory potential recorded from the human scalp," *Proceedings of the National Academy of Sciences*, vol. 78, no. 4, pp. 2643–2647, 1981.

[13] J. Pan and W. Tompkins, "A real-time QRS detection algorithm," *IEEE Transactions on Biomedical Engineering*, vol. 3, pp. 230–236, 1985.

[14] J. Catalano, *Guide to ECG analysis*, 2nd ed. Lippincott Williams & Wilkins, 2002.

[15] V. Goverdovsky, D. Looney, P. Kidmose, C. Papavassiliou, and D. P. Mandic, "Co-Located multimodal sensing: A next generation solution for wearable health," *IEEE Sensors Journal*, vol. 15, no. 1, pp. 138–145, 2015.